Symmetry breaking in a turbulent environment

Alexandros Alexakis and François Pétrélis
Laboratoire de Physique de l'École Normale Supérieure, CNRS, PSL Research University, Sorbonne Université, Université de Paris, F-75005 Paris, France

Santiago J. Benavides
Department of Earth, Atmospheric, and Planetary Sciences, Massachusetts Institute of Technology, Cambridge, Massachusetts 02139, USA

Kannabiran Seshasayanan
Service de Physique de l'Etat Condensé, CNRS UMR 3680, CEA Saclay, 91191 Gif-sur-Yvette, France and Department of Physics, Indian Institute of Technology Kharagpur, Kharagpur 721 302, India

(Received 19 April 2020; accepted 28 January 2021; published 15 February 2021)

In this work we investigate symmetry breaking in the presence of a turbulent environment. The transition from a symmetric state to a symmetry-breaking state is demonstrated using two examples: (1) the transition of a two-dimensional flow to a three-dimensional flow as the fluid layer thickness is varied and (2) the dynamo instability in a thin layer flow as the magnetic Reynolds number is varied. We show that these examples have similar critical exponents that differ from the mean-field predictions. The critical behavior can be related to the multiplicative nature of the fluctuations and can be predicted in certain limits using results from the statistical properties of random interfaces. Our results indicate the possibility of existence of a new class of out-of-equilibrium phase transition controlled by the multiplicative noise.

DOI: 10.1103/PhysRevFluids.6.024605

I. INTRODUCTION

Phase transitions are ubiquitous in nature. The liquid-gas transition or the transition from a magnetized to a nonmagnetized state in ferromagnetic materials are textbook examples [1–3]. Critical phenomena of continuous phase transitions have been a major research topic for more than 50 years. It is now well understood that, at equilibrium, the thermal fluctuations play a dominant role: the amplitude of the order parameter, say, A, depends on the distance from the critical point, say, μ, as a power law $A \propto \mu^{\beta}$ where the value of the exponent β differs from the mean-field prediction obtained when thermal fluctuations are neglected. These results are verified in experiments and are understood theoretically for instance through renormalization methods. In contrast, the behavior of critical phenomena in nonequilibrium systems remains less well understood. In liquid crystals, a transition between two topologically different nematic phases was shown to belong to the class of directed percolation [4]. The transition from the laminar state to turbulence in extended shear flows [5–7] is an out-of-equilibrium phase transition that also belongs to the directed percolation universality class. Here we consider examples of bifurcations over a turbulent flow, in which the system transitions from a state that respects a certain symmetry to a different state where this symmetry is broken. We need to emphasize that the transition is from a turbulent/chaotic state to another turbulent state, and thus it differs from the classical laminar to turbulent transition.

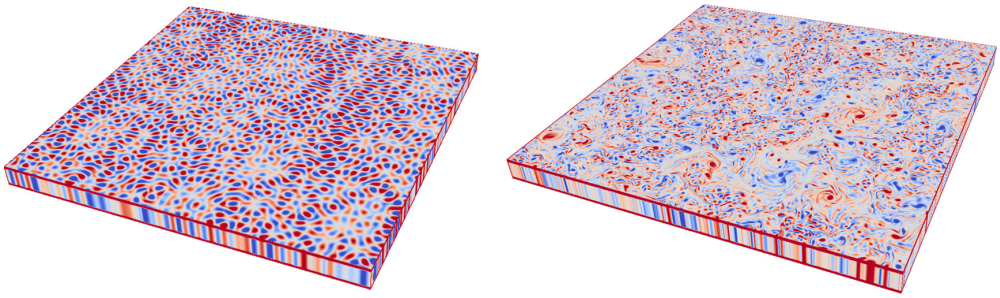

FIG. 1. Vertical vorticity, $\omega_z = \hat{z} \cdot (\nabla \times \overline{\mathbf{u}})$, of the 2D field for a random (left) and a turbulent state (right).

Furthermore, the symmetries and the nature of the coupling of the turbulent fluctuations differ from the former examples, indicating the possibility of a new universality class.

The first system that we consider is a two-dimensional (2D) flow which undergoes an instability towards a three-dimensional (3D) flow. The nature of the transition from a 2D to a 3D flow is a challenging topic of wide-ranging interest in turbulence [8]. It is a common situation in geophysics as rotation and the small pressure scale height of planetary atmospheres tend to bidimensionalize the flows [9,10]. Here we consider an idealized flow confined in a thin layer of thickness H in the normal z direction and of width $L \gg H$ in the in-plane x and y directions with free slip boundary conditions in z and periodic boundary conditions in x and y. The flow is described by the incompressible velocity $\mathbf{u}$ that follows the Navier-Stokes equations,

$$\partial_t \mathbf{u} + \mathbf{u} \cdot \nabla \mathbf{u} = -\nabla P + \nu \nabla^2 \mathbf{u} - \alpha \overline{\mathbf{u}} + \mathbf{f}, \tag{1}$$

where P is the pressure, ν is the kinematic viscosity, and α is a drag coefficient that acts only on the vertically averaged part of the flow, denoted by $\overline{\mathbf{u}}$, used to model Ekman friction [11]. Energy is injected by $\mathbf{f}$, a random delta-correlated in time forcing, with a fixed averaged energy injection rate ϵ, an input parameter. It is 2D, depending only on x and y, so that $\overline{\mathbf{f}} = \mathbf{f}$, and acts only on the horizontal components. It is acting at some length scale ℓ, such that $H \ll \ell \ll L$. The injection rate ϵ and the length scale ℓ will be used to nondimensionalize our system and will be set accordingly to unity. The part of the flow that varies along the vertical direction is denoted as $\tilde{\mathbf{u}} = \mathbf{u} - \overline{\mathbf{u}}$ and follows the equation

$$\partial_t \tilde{\mathbf{u}} + \overline{\mathbf{u}} \cdot \nabla \tilde{\mathbf{u}} + \tilde{\mathbf{u}} \cdot \nabla \overline{\mathbf{u}} = \overline{\tilde{\mathbf{u}} \cdot \nabla \tilde{\mathbf{u}}} - \tilde{\mathbf{u}} \cdot \nabla \tilde{\mathbf{u}} - \nabla \tilde{P} + \nu \nabla^2 \tilde{\mathbf{u}}. \tag{2}$$

Note that because $\overline{\mathbf{f}} = \mathbf{f}$ the velocity variation $\tilde{\mathbf{u}}$ is not directly forced, so that $\tilde{\mathbf{u}} = 0$ is always a solution of the system. For very thin layers and close to the onset of the instability $\tilde{\mathbf{u}}$ can be approximated with one Fourier mode in the z direction as in Ref. [12].

For small H a purely 2D flow is generated, for which the velocity field is planar and invariant under translation across the layer. Its dynamics is determined by the value of the Reynolds numbers $\mathrm{Re} = \epsilon^{1/3} \ell^{4/3} / \nu$ and $R_\alpha = \epsilon^{1/3} / \alpha \ell^{2/3}$. For small Re and R_α the flow is random following the statistical properties of the forcing with Gaussian fluctuations, and a limited range of length scales excited. In contrast, for large values of Re and R_α the flow is turbulent, and a cascade develops leading to fluctuations with non-Gaussian statistics distributed over a wide range of scales. We will refer to these limiting cases as *random* and *turbulent*, respectively. A snapshot of the vertical vorticity, $\omega_z = \hat{z} \cdot (\nabla \times \overline{\mathbf{u}})$, is displayed in Fig. 1 for a random (left panel) and a turbulent (right panel) state. In both cases, the fluctuations do not depend on the vertical coordinate, and the system is invariant in this direction $\tilde{\mathbf{u}} = \mathbf{0}$. If, however, H is increased, the flow breaks this symmetry and 3D variations become unstable $\tilde{\mathbf{u}} \neq 0$. The system thus changes from a phase where $\tilde{\mathbf{u}} = \mathbf{0}$ pointwise to a phase where $\tilde{\mathbf{u}} \neq 0$ at a critical height that is shown to scale like $H \propto \ell\, \mathrm{Re}^{-1/2}$ [12]. In this system we use as control parameter μ the normalized height of the layer $\mu = H/\ell$, while the order parameter is characterized by the different moments of the 3D fluctuations $A_m = \langle |\tilde{\mathbf{u}}|^m \rangle$

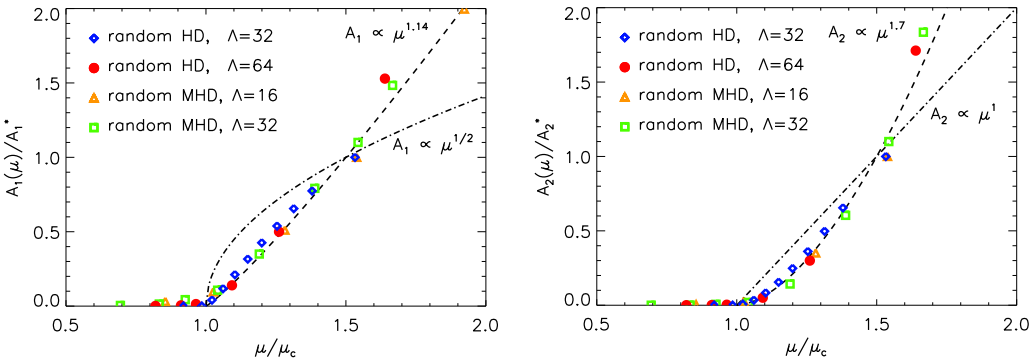

FIG. 2. First and second moment A_1, A_2 for both the hydrodynamic problem and the MHD problem and for a random flow and different values of Λ. The y axis is normalized by $A_m^* = A_m(3\mu_c/2)$.

where the angular brackets stand for space-time averaging. The size of the system is measured by the parameter $\Lambda = L/\ell$.

The second system that we investigate is the dynamo instability of a swirling electrically conducting fluid transitioning from an unmagnetized to a magnetized state [13]. The system is governed by the equations of magnetohydrodynamics (MHD)

$$\partial_t \mathbf{u} + \mathbf{u}\cdot\boldsymbol{\nabla}\mathbf{u} = -\boldsymbol{\nabla}P + \nu\nabla^2\mathbf{u} - \alpha\overline{\mathbf{u}} + \mathbf{b}\cdot\boldsymbol{\nabla}\mathbf{b} + \mathbf{f} \tag{3}$$

$$\partial_t \mathbf{b} + \mathbf{u}\cdot\boldsymbol{\nabla}\mathbf{b} = \mathbf{b}\cdot\boldsymbol{\nabla}\mathbf{u} + \eta\nabla^2\mathbf{b} \tag{4}$$

where $\mathbf{b}$ is the magnetic field and η the magnetic diffusivity. As in the previous case the considered flow is confined in a thin layer, here with triple periodic boundary conditions. It is important to note that in the absence of the third component no dynamo instability exists. For this reason, although the forcing is invariant along the z direction as before, all three components are present in $\mathbf{f}$ for this problem [i.e., two-dimensional, three-component (2D3C)]. It is again random and injects energy at a typical length ℓ at rate ϵ. The ratio of the energy injection rate in the transverse component ϵ_v to the energy injection rate in the in-plane directions ϵ_h is measured by $\gamma = \epsilon_v/\epsilon_h$. The layer thickness H is sufficiently thin so that the flow remains 2D3C $\mathbf{u} = \overline{\mathbf{u}}$, while it is thick enough so that a single Fourier mode of the magnetic field becomes unstable $\mathbf{b}(x, y, z, t) = \tilde{\mathbf{b}}(x, y, t)e^{i2\pi z/H}$ as in Refs. [14,15]. Keeping, Re, R_α, and Λ (defined as before) fixed we use the magnetic Reynolds number $\mu = Rm = \epsilon_h^{1/3}\ell^{4/3}/\eta$ as control parameter and as order parameter the different moments of the magnetic field $A_m = \langle|\tilde{\mathbf{b}}|^m\rangle$. The two systems are numerically simulated using codes described in Refs. [12,15] on a 2048^2 grid. The simulations were run until a statistically steady state is reached in which the different moments are measured.

We begin by examining the random flow, for which $\mathrm{Re} \simeq R_\alpha \simeq 1$, depicted in the left panel of Fig. 1. The amplitudes A_1 and A_2 are displayed in Fig. 2 as a function of μ for the hydrodynamic model (HD) and the MHD model with $\gamma = 4$, for different values of Λ. For both systems the first and the second moments collapse on a single master curve. Independence of the data on Λ also indicates that the large box limit has been reached. As a consequence both systems appear to have the same critical behavior, suggesting a possibility that they belong to the same universality class. The moments bifurcate from zero at a critical value $\mu = \mu_c$ and scale with $\mu - \mu_c$ as power laws: $A_1 \propto (\mu - \mu_c)^{\beta_1}$ and $A_2 \propto (\mu - \mu_c)^{\beta_2}$. An accurate estimate of the value of the exponents β_1, β_2 is difficult to obtain. For these turbulent systems, the existence of low-frequency velocity fluctuations renders the situation difficult as statistical convergence requires very long simulations. However, one can say with confidence that they clearly differ from $\beta_1 = 1/2$ and $\beta_2 = 1$, which are the exponents obtained for static fields, or by mean-field predictions where the small-scale fluctuations are modeled by transport coefficients like an eddy diffusivity or an α coefficient [16]. They also

differ from the zero-dimensional $d = 0$ bifurcations in the presence of multiplicative noise, which is termed on-off intermittency and leads to $\beta_1 = \beta_2 = 1$ [17,18].

In order to explain these new exponents and to identify and characterize the universality class of these systems, we resort to deriving a field equation, modeling the approximate equations of motion for the amplitude of the unstable $\tilde{\mathbf{u}}$ and $\mathbf{b}$ near the threshold of instability. This derivation will be based on symmetries of the bifurcating system.

The hydrodynamic problem is symmetric under reflection in the $z = 0$ plane, which we denote by $\mathcal{S}$. Once μ goes beyond the critical value, the first linearly unstable vertical mode breaks this planar symmetry and is thus odd under $\mathcal{S}$. If we denote this solution $\tilde{\mathbf{u}} = \phi(x, y, t)\mathbf{v_u}$, where ϕ is the amplitude of the unstable mode and $\mathbf{v_u}$ is the vertical mode structure, then we have that $\mathcal{S}\mathbf{v_u} = -\mathbf{v_u}$. Because the hydrodynamic problem is symmetric under reflection, if $\phi\mathbf{v_u}$ is a solution, then $\mathcal{S}\phi\mathbf{v_u} = -\phi\mathbf{v_u}$ is also a solution. In other words ϕ and $-\phi$ are solutions of the problem. Similarly, for the magnetic problem, because of the invariance of the MHD equation under change of sign of the magnetic field, if $\mathbf{b}$ is a solution so is $-\mathbf{b}$. With the same reasoning let $\mathbf{b_u}$ be the linearly unstable mode and ϕ its amplitude; if $\phi\mathbf{b_u}$ is a solution, so is $-\phi\mathbf{b_u}$. It is important to notice that these symmetries are satisfied even taking into account the turbulent fluctuations. Therefore when modeling the effect of the turbulent fluctuations in the field equation by stochastic terms, only odd terms in ϕ appear. Accordingly, the first-order term in ϕ that couples to the spatiotemporal fluctuations of the background field is linear. The symmetries of the problem thus imply that the noise acting on the perturbation field is multiplicative. For the same reason, the lowest order nonlinear term is cubic.

We thus end with the following field equation:

$$\frac{\partial \phi}{\partial t} = \mu\phi - C\phi^3 + D\nabla^2\phi + \zeta(\mathbf{x}, t)\phi, \tag{5}$$

where ζ is spatiotemporal noise (interpreted in the Stratonovich sense), μ is the control parameter, and C, D are constants. Here the term $\zeta(\mathbf{x}, t)\phi$ expresses the local amplification or decrease effects, while $\mu\phi$ expresses their mean counterparts. The nonlinearity $-C\phi^3$ is responsible for saturating the growth. The term $D\nabla^2\phi$ is responsible for diffusing any localized structure of ϕ. This equation has been studied to model, for instance, chemical reactions or synchronization transition [19–21].

When ζ is white and Gaussian, renormalization group methods allow one to predict the critical behavior of the system. For a space of dimension $d \leqslant 2$, a transition exists between an absorbing phase where $\phi = 0$ and an active phase where $\phi \neq 0$. Close to the critical point, the field scales as $\langle|\phi|^n\rangle = (\mu - \mu_c)^{\beta_n}$. It has been shown [22] that some critical exponents of Eq. (5) can be related to the exponents of the Kardar-Parisi-Zhang equation (KPZ) [23,24]. Indeed, the linear part of Eq. (5) is transformed by the Cole-Hopf transformation into the KPZ equation. This equation describes the growth of a random surface when nonlinear effects are taken into account. Some predictions of the KPZ equation are thus useful for the systems that we are considering. For $d = 2$ and white noise, the exponents β_n have been calculated numerically: $\beta_1 \simeq 1.14$ and $\beta_2 \simeq 1.7$ [25]. These predictions are displayed in Fig. 2 and are compatible with the results obtained for the two systems under study.

The behavior of the different moments A_m results from the spatial distribution of the unstable field ($\tilde{\mathbf{u}}$, $\mathbf{b}$, ϕ). In the top panels (a) of Fig. 3 five snapshots of the energy density of the field $\tilde{\mathbf{u}}$ are shown for different values of μ. The snapshots correspond to the data marked by blue diamonds in Fig. 2. Far from the onset (rightmost panels) the unstable field is spread throughout the domain. As μ comes closer to the onset the unstable field becomes more sparse occupying a smaller and smaller fraction of the domain. Very close to the onset (leftmost panel) only a few structures are left, and in most of the domain the unstable field is almost zero. In Fig. 3(b) a series is shown for solutions of Eq. (5) that shows similar features.

There are a few remarks that need to be made here. First, we stress that the predictions for the field equation (5) hold for the limit of infinite domain size $\Lambda \to \infty$. For finite domains these exponents can be contaminated by finite-size effects [26]. One can see, for example, from Eq. (5) that when the inverse diffusion timescale L^2/D is much smaller than the growth rate fluctuations,

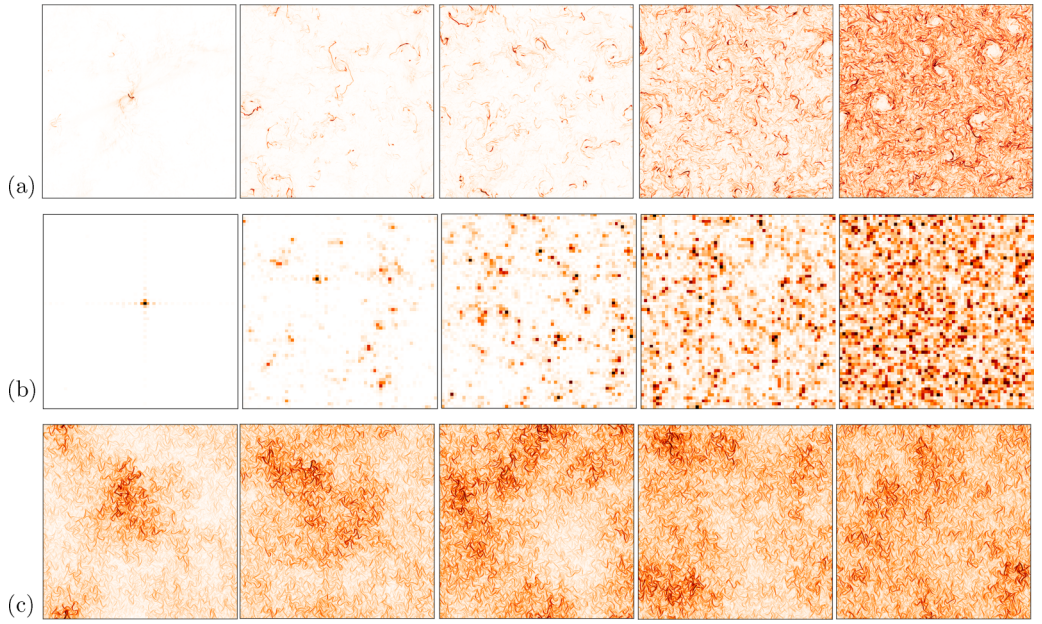

FIG. 3. For increasing values of μ (from left to right and starting from close to μ_c) the images display the following: (a) energy density of 3D velocity field for the random base flow for the data points displayed in Fig. 2; (b) energy density of the field ϕ for the field equation (5) with white noise solved on a 64×64 grid; and (c) energy density of magnetic field energy for the data points displayed in Fig. 4.

the spatial fluctuations are averaged out and the system recovers the mean-field behavior. This limitation has profound implications on the systems under study because the domain size is always finite and diffusion is controlled by eddy diffusion that in general has nontrivial dependency with the system control parameters. For example, in the MHD system when we decrease the parameter γ we decrease the growth rate, which depends on the product of vertical and horizontal velocity components, while we increase the turbulent diffusivity, which depends only on the horizontal components. As a result the system becomes much more diffusive as γ is decreased. In Fig. 4 we show the behavior of A_1 for the dynamo problem as in Fig. 2 but with a smaller value of $\gamma = 1$. The

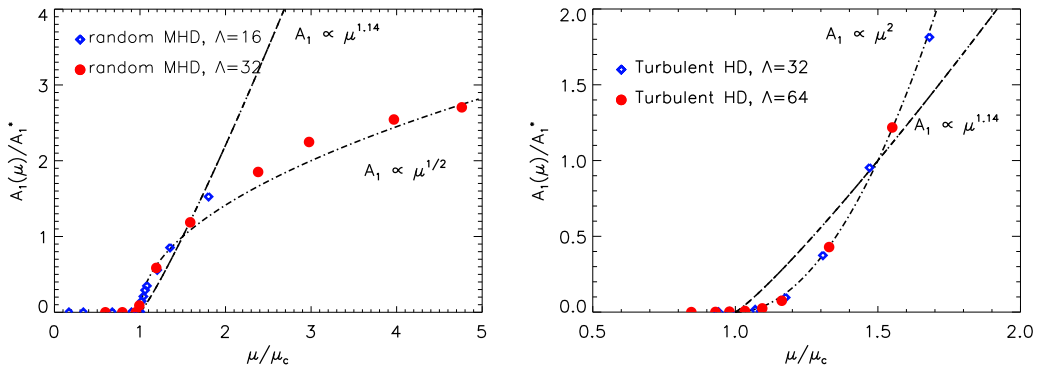

FIG. 4. Left panel: First moment A_1 for the thin layer dynamo problem for $\gamma = 1$ for which turbulent diffusion is much more effective than in the case of Fig. 2. Right panel: First moment A_1 for the thin layer problem for the turbulent flow.

anomalous exponent observed in Fig. 2 is not present in the case of the left panel of Fig. 4, and the data are much better fitted with the mean-field exponent $\beta_1 = 1/2$. Similarly the second moment A_2 (not plotted) here is much closer to $\beta_2 = 1$. Finally, the energy distribution shown in Fig. 3(c) does not show the spatial distribution observed in the other panels. This observed mean-field behavior is, however, due to finite-size effects. The anomalous scaling, and the associated intense localization of the field, are expected to be recovered in a larger system $\Lambda \to \infty$.

Furthermore, the predicted exponents based on Eq. (5) are valid when the noise is white. Their values differ when the noise has different properties (see, for instance, Ref. [24], p. 285, and Refs. [27,28]). Indeed, when we simulate Eq. (5) with colored noise larger exponents are observed. The value of the measured exponents appeared to depend on the spectral properties of the noise. This is important because in turbulent flows the spatiotemporal correlations of the fluctuations are far from being white and Gaussian. In contrast to the random flow for which the fluctuations are localized in scale, the energy cascade in the turbulent system leads to fluctuations across a wide range of scales. The exponents measured for the fully turbulent flow, such as the one depicted in the right panel of Fig. 1, thus differ from the predictions of Eq. (5) with a white noise. In the right panel of Fig. 4, A_1 is displayed as a function of μ for the hydrodynamic model in the turbulent state with $\mathrm{Re} \simeq 100$, $R_\alpha \simeq 30$ and for the same values of Λ as in Fig. 2. The data overlap again in one master curve. The measured exponent is larger than both the mean-field prediction and the prediction of the white noise model of Eq. (5) and is closer to $\beta_1 \simeq 2$. Theoretical predictions for Eq. (5) in two dimensions with colored noise are still limited. Understanding the precise value of these exponents from properties of the KPZ equations subject to colored spatiotemporal noise related to the spectral properties of turbulent flows would be of great interest. Results for KPZ in two dimensions are still limited, but in one dimension, it is known that the roughness exponent (χ with the notation of Ref. [22]) increases with the slope ρ of the noise spectrum (assumed to be of the form $k^{-2\rho}$). Assuming that this remains true in two dimensions, and using the known scaling relations for the problem of multiplicative noise [22], we expect that the exponent β is larger when ρ is large (for a turbulent flow and a noise term proportional to the velocity gradient $\rho = 1/3$) than when the noise is white ($\rho = 0$), which has same exponent as in the case of the random flow. Thus the exponent can be sensitive to the spatial properties of the turbulent fluctuations and in particular the existence of an inverse cascade.

Furthermore, the universality class can depend on the vectorial or scalar form of the bifurcating field [20]. In the examined cases it is a vector for the two physical systems. For the field equation we have observed qualitatively similar results for both a 2D vectorial and a scalar field. Further work and investigations are of course in order to clarify if there are differences in this case too that could not be resolved by the present data.

Finally we note that the considered systems are essentially 2D, and we expect that 3D systems belong to different universality classes. Further investigations of field equations such as Eq. (5) are required to determine the role of the dimension of space and of the order parameter, as well as finite-size effects and long-temporal and long-spatial noise correlation effects. Further numerical but also experimental investigations are also indispensable for clarifying all aspects of this transition. We believe that the results presented in this article open new directions for the study of a variety of instabilities occurring over a turbulent system such as in turbulent atmospheric layers, surface waves driven by turbulent winds in the ocean, and magnetic dynamo field generation in stars driven by turbulent convection.

ACKNOWLEDGMENTS

This work was granted access to the HPC resources of MesoPSL financed by the Region Ile de France and the project Equip@Meso (reference ANR-10-EQPX-29-01) of the program Investissements d'Avenir supervised by the Agence Nationale pour la Recherche and the HPC resources of GENCI-TGCC and GENCI-CINES (Project No. A0070506421) where the present numerical simulations have been performed. This work has also been supported by the Agence

nationale de la recherche (ANR DYSTURB project No. ANR17-CE30-0004). S.J.B. acknowledges funding from a grant from the National Science Foundation (OCE-1459702).

[1] S. K. Ma, *Modern Theory of Critical Phenomena Frontiers in Physics* (Benjamin, Reading, MA, 1976).
[2] N. Goldenfeld, *Lectures on Phase Transitions and the Renormalization Group Frontiers in Physics* (Westview Press, Boulder, 1992).
[3] J. Zinn-Justin, *Quantum Field Theory and Critical Phenomena*, International Series of Monographs on Physics Vol. 113 (Clarendon Press, Oxford, 2002).
[4] K. A. Takeuchi, M. Kuroda, H. Chaté, and M. Sano, Directed Percolation Criticality in Turbulent Liquid Crystals, Phys. Rev. Lett. **99**, 234503 (2007).
[5] G. Lemoult, L. Shi, K. Avila, S. V. Jalikop, M. Avila, and B. Hof, Directed percolation phase transition to sustained turbulence in Couette flow, Nat. Phys. **12**, 254 (2016).
[6] M. Sano and K. Tamai, A universal transition to turbulence in channel flow, Nat. Phys. **12**, 249 (2016).
[7] M. Chantry, L. S. Tuckerman, and D. Barkley, Universal continuous transition to turbulence in a planar shear flow, J. Fluid Mech. **824**, R1 (2017).
[8] A. Alexakis and L. Biferale, Cascades and transitions in turbulent flows, Phys. Rep. **767**, 1 (2018).
[9] D. Byrne and J. A. Zhang, Height-dependent transition from 3-D to 2-D turbulence in the hurricane boundary layer, Geophys. Res. Lett. **40**, 1439 (2013).
[10] R. M. B. Young and P. L. Read, Forward and inverse kinetic energy cascades in Jupiter's turbulent weather layer, Nat. Phys. **13**, 1135 (2017).
[11] J. Pedlosky, *Geophysical Fluid Dynamics* (Springer-Verlag, New York, 1987).
[12] S. J. Benavides and A. Alexakis, Critical transitions in thin layer turbulence, J. Fluid Mech. **822**, 364 (2017).
[13] H. K. Moffatt, *Magnetic Field Generation in Electrically Conducting Fluids* (Cambridge University Press, 1978).
[14] K. Seshasayanan and F. Pétrélis, Growth rate distribution and intermittency in kinematic turbulent dynamos: Which moment predicts the dynamo onset? Europhys. Lett. **122**, 64004 (2018).
[15] K. Seshasayanan, B. Gallet, and A. Alexakis, Transition to Turbulent Dynamo Saturation, Phys. Rev. Lett. **119**, 204503 (2017).
[16] A. Alexakis, S. Fauve, C. Gissinger, and F. Pétrélis, Effect of fluctuations on mean-field dynamos, J. Plasma Phys. **84**, 735840401 (2018).
[17] H. Fujisaka and T. Yamada, A new intermittency in coupled dynamical systems, Prog. Theor. Phys. **74**, 918 (1985).
[18] N. Platt, E. A. Spiegel, and C. Tresser, On-Off Intermittency: A Mechanism for Bursting, Phys. Rev. Lett. **70**, 279 (1993).
[19] M. A. Munoz, Multiplicative noise in non-equilibrium phase transitions: A tutorial, arXiv:cond-mat/0303650 (2003).
[20] U. C. Täuber, *Critical dynamics: A Field Theory Approach to Equilibrium and Non-equilibrium Scaling Behavior* (Cambridge University Press, 2014).
[21] M. Henkel, H. Hinrichsen, S. Lübeck, and M. Pleimling, *Non-equilibrium Phase Transitions*, Vol. 1 (Springer, 2008).
[22] Y. Tu, G. Grinstein, and M. A. Muñoz, Systems with Multiplicative Noise: Critical Behavior from KPZ Equation and Numerics, Phys. Rev. Lett. **78**, 274 (1997).
[23] M. Kardar, G. Parisi, and Y.-C. Zhang, Dynamic Scaling of Growing Interfaces, Phys. Rev. Lett. **56**, 889 (1986).
[24] T. Halpin-Healy and Y.-C. Zhang, Kinetic roughening phenomena, stochastic growth, directed polymers and all that: Aspects of multidisciplinary statistical mechanics, Phys. Rep. **254**, 215 (1995).
[25] W. Genovese, M. A. Muñoz, and J. M. Sancho, Nonequilibrium transitions induced by multiplicative noise, Phys. Rev. E **57**, R2495 (1998).

[26] Barber, M. N., in *Phase Transitions and Critical Phenomena*, edited by C. Domb and J. L. Leibovitz (Academic, London, 1983), Vol. 8, pp. 146–259.
[27] F. Pétrélis and A. Alexakis, Anomalous Exponents at the Onset of an Instability, Phys. Rev. Lett. **108**, 014501 (2012).
[28] A. Alexakis and F. Pétrélis, Critical exponents in zero dimensions, J. Stat. Phys. **149**, 738 (2012).